Enhanced Voltage-Frequency Control Method for Induction Motor

Ioan Iov Incze, Maria Imecs, Csaba Szabo
Department of Electrical Drives and Robots
Technical University of Cluj-Napoca
C. Daicoviciu str. 15, RO-600020, Cluj-Napoca
Romania
ioan.incze@edr.utcluj.ro, imecs@edr.utcluj.ro, csaba.szabo@edr.utcluj.ro

Abstract – **The popular "constant Volt/Hertz" control method's backdraw is the lost of torque capability at low speed. This is caused by stator voltage drops that at reduced frequencies are comparable as magnitude with the supply voltage. More techniques are known to eliminate this undesirable effect. The best results are obtained by vectorial compensation of the resistive-voltage losses. The compensation applied also to the reactive-voltage drop described in this paper, offer further improvements of the induction motor torque capabilities. The paper also investigates the computation of the voltage angle- and amplitude-reference by the current-feedback-based method. Different approaches are presented, among others the current-dependent slope characteristics are especially discussed in detail. MATLAB-Simulink simulation of a vectorial compensated current-feedback-based system was performed, followed by experimental investigation. The description of the test rig is also given, which is based on a dSPACE DS1104 controller board. Conclusions and references are presented.**

I. INTRODUCTION

The use of inverters in controlled AC drives ensure economical (loss-less) operation. With the so-called "constant Volt/Hertz" (known also as U/f = constant) method it can be achieved the indirect and empirical stator-flux control. (i.e. $\Psi_s \cong$ ct.). Since the introduction of the field-orientation principle and the technological advances in domain of AC motor control, the main research was concentrated on vector control area. In spite of this fact, the scalar control methods still presents some interest, with problems waiting to be solved at low speed operation. To achieve the highest possible torque per amper capability of the stator current, which ensures an optimal use of drive capabilities, the stator-flux magnitude has to be kept constant at the rated value. This requirement can be made by adjusting the ratio between the magnitude (U_s) and the frequency (f_s) of the stator voltage.

Fig. 1 presents a basic control scheme of the U/f procedure. From the reference frequency f_s^{Ref}, the angular frequency $\Omega_s=2\pi f_s$ and the amplitude of the reference stator voltage vector U_s^{Ref} are calculated. The three-phase voltage reference signals will be generated by the "Sine-Wave Generator" block. The simplest procedure does not includes any feedback quantities, and the reference voltage was usually computed as:

$$U_s^{Ref} = U_{sN} \frac{f_s^{Ref}}{f_{sN}}. \quad (1)$$

Based on experimental results, it can be concluded, that this simple procedure works satisfactory below and slightly above the rated speed. However, above rated speed, the supply voltage cannot be increased and the flux linkage value will decrease (i.e. the field-weakening region). For this reason this scalar control method, in order to maintain the constant flux operation, is applied only at rated frequency and below.

At low speed the voltage drop on the stator reactance became comparable as magnitude with the applied voltage. The flux will decrease, and the machine torque capability will be much smaller as well. For a better operation this voltage drop has to be compensated. The effect of this neglected voltage-drop is as more important as the ratio $a_s = X_s/R_s$ is reduced [6]. Above $X_s = \Omega_s L_s$, where R_s is the stator resistance and $L_s = (L_m + L_{\sigma s})$ is the resultant three-phase inductance, including also the leakage component.

In order to compensate the effect of these voltage drops at low speeds, different techniques were developed to provide more voltage to the motor than the previously presented simple procedure. This techniques are:

- Programmed voltage-frequency characteristics [1];
- Formula-based voltage-drop compensation [6], [10];
- Current-feedback-based voltage-drop compensation [1], [3], [5].

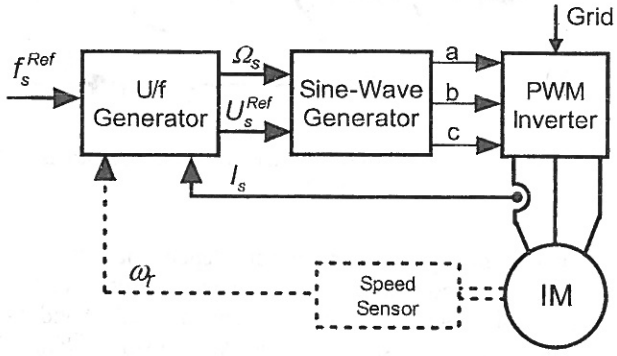

Fig. 1. Basic configuration of a scalar induction motor drive system, based on the Volt/Hertz principle

In the case of programmed voltage-frequency characteristics a supplementary constant voltage is added at low frequencies. This method has its disadvantage that at no-load condition over excitation occurs at low speeds. The formula-based voltage-drop compensation method computes the corresponding voltage reference based on imposed frequency and motor parameters, only. The computation formula is derived from the steady-state equivalent circuit of the motor. In the both cases is ignored the voltage dependence on the load. For current-feedback-based voltage-drop compensation the voltage value is computed taking into account also the motor actual current, making thus the prescribed voltage reference load-dependent.

An other voltage-drop compensation technique takes into account the vectorial position of the voltage drop phasor. This vectorial compensation of stator-voltage drop offers more accurate performance [7]. In this case the computational effort is considerable increased. Refined Volt/Hertz techniques apply load-dependent compensation of stator-voltage drop. In this paper there are developed the current-feedback-based voltage-drop compensation methods.

II. SCALAR COMPENSATION OF THE STATOR RESISTIVE VOLTAGE DROP

There are known several approaches, which are based on adding to the stator-voltage a component proportional to the measured stator-current.

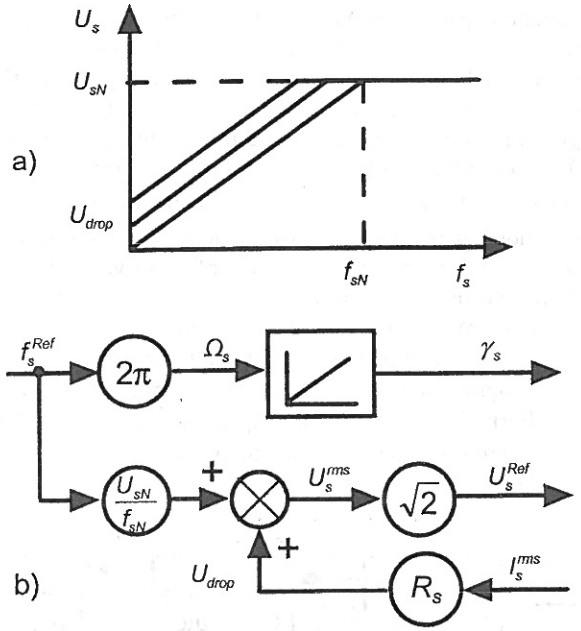

Fig. 2. Current compensated *U/f* procedure with shifted characteristics (a) and structure (b)

In a simple approach the current-dependent voltage drop component is computed as $R_s i_s$, where i_s represents the rms value of the actual stator current. This method provides the torque even if the speed is low. At no-load running, the machine is still over-exited, because the magnetizing current is treated as load current. The compensation is also inadequate in regenerative operation.

In Fig. 2 are presented the control characteristics, which are parallel shifted. Due to the parallel up-shifting of voltage-frequency characteristics the voltage-limitation (at the rated voltage U_{sN}) is achieved at lower frequencies than the rated frequency f_{sN}, which fact is leading to an inadequate compensation in this upper speed region.

To improve the above described drawbacks, an other approach is proposed, based on the phase-sensitive rectifying, using as reference the voltage of a stator-phase in order to identify the active component of the stator-current. The current component, which is in phase with the voltage will be used for voltage boost computing [1].

This inaccuracy may be avoided by current-dependent modification of the characteristics slope as is shown in Fig. 3,a. That is performed by computing the voltage reference according to the following relation [3]:

$$U_s^{Ref} = \sqrt{2}\left(R_s I_s^{rms} + \frac{U_{sN}^{rms} - R_s I_s^{rms}}{f_{sN}} f_s^{Ref} \right), \quad (2)$$

where the current dependent slope is:

$$\sqrt{2}\left(\frac{U_{sN}^{rms} - R_s I_s^{rms}}{f_{sN}} \right). \quad (3)$$

Fig. 3.b) presents the computing structure of the angle- and amplitude-reference for stator-voltage generation based on (2).

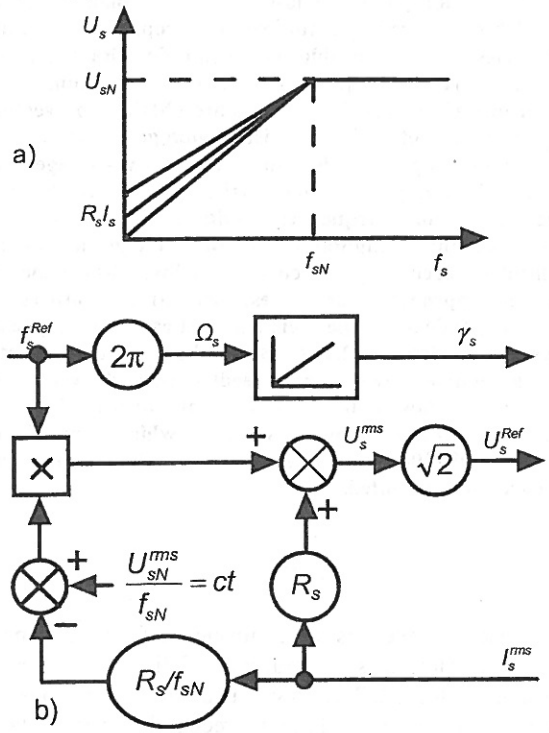

Fig. 3. Current compensated *U/f* procedure with modified slope of characteristics (a) and structure (b)

The mathematical calculi involved in voltage computation are simple. They may be performed even by means of low-end microcontrollers, supporting low cost applications.

III. VECTORIAL COMPENSATION OF THE STATOR RESISTIVE VOLTAGE DROP

An improved method was introduced in [7]. The compensation of the stator resistance voltage drop, and is realized by vectorial adding it to the supply voltage. One of the advantages of this method is that it requires only a minimum set of the motor parameters and the measurement of the stator currents.

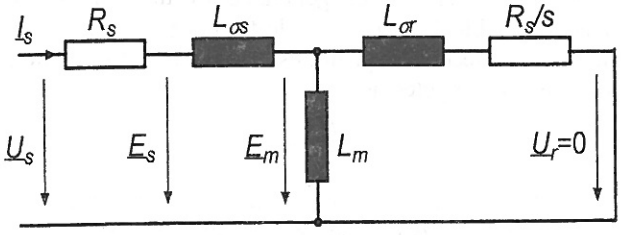

Fig. 4. Steady-state equivalent circuit of the induction motor

Fig. 4 presents the induction motor steady-state equivalent circuit. The phasor diagram of the stator-circuit used for this particular control procedure is presented in Fig. 5.

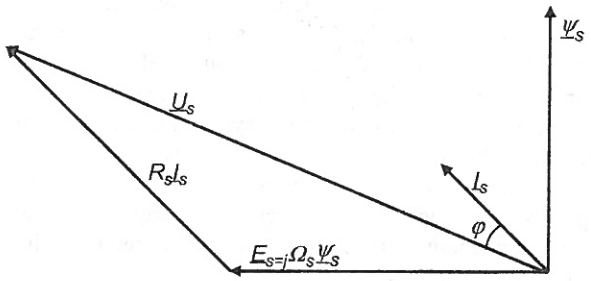

Fig. 5. Phasor diagram used for R_s compensation

Based on Fig. 5, the magnitude of the e.m.f. E_s is computed as:

$$E_s^2 = \left(U_s^2\right) + \left(R_s I_s\right)^2 - 2U_s\left(R_s I_s\right)\cos\varphi \qquad (4)$$

At rated working point the steady-state magnitude of the E_s is defined as E_{sN}. At any f_s frequency to ensure the constant U/f operation, his value will be computed as $\frac{E_{sN} f_s}{f_{sN}}$. By substituting this in the previous equation, the stator voltage can be computed as:

$$U_s = R_s I_s \cos\varphi + \sqrt{\left(\frac{E_{sN} f_s}{f_{sN}}\right) - \left(R_s I_s\right)^2 (\sin\varphi)^2} \qquad (5)$$

The sinφ and cosφ terms are obtained by on-line computation as the phase difference between the stator current and voltage vectors, using two vector analyzers, and a coordinate transformation [12]. They are considered already common blocks in vector control systems. Using this voltage-drop compensation method, the torque capability of the induction machine is substantially improved. It can be observed on the mechanical (torque-speed) static characteristics. The main advantage lies not only in the increased breakdown torque, but also in extension of the linear section of the static characteristic, where the drive usually works. From simulation results we observed that using this compensation method, at the rated load torque the stator current is maintained at his rated value.

IV. VECTORIAL COMPENSATION OF THE STATOR RESISTIVE AND REACTIVE VOLTAGE DROP

By analysing different types of induction machines, it can be observed, that the voltage drop due to the stator leakage reactance $X_{\sigma s}$ is significant, and in some cases comparably or greater than the stator resistance, even at low frequencies. This fact leads to the conclusion that also this voltage drop should be compensated.

An analysis of the $X_{\sigma s}/R_s$ ratio versus f_s frequency for different types of induction motors is presented in Fig. 6.

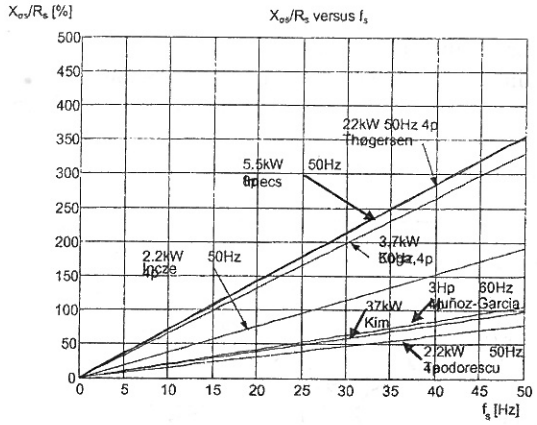

Fig. 6. $X_{\sigma s}/R_s$ dependency versus stator frequency for different types of induction motors

In Fig. 7 the modified phasor diagram is presented for for indirect air-gap field control by compensation of the resistive and reactive voltage drop. Based on this diagram the e.m.f. E_m can be expressed as:

$$E_m^2 = \left(\frac{E_{mN} f_s}{f_{sN}}\right)^2 - \left(\left(R_s I_s\right) - \frac{\Omega_s L_{\sigma s} I_s}{\sin\varphi}\cos\varphi\right)^2 \sin^2\varphi + \left(R_s I_s - \frac{\Omega_s L_{\sigma s} I_s}{\sin\varphi}\cos\varphi\right)\cos\varphi\sin^2\varphi \qquad (6)$$

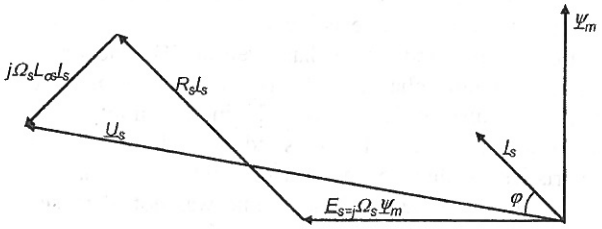

Fig. 7. Phasor diagram for R_s and $X_{\sigma s}$ compensation

The stator voltage for Ψ_m = ct. will be calculated as follows:

$$U_s = \frac{\Omega_s L_{\sigma s} I_s}{\sin\varphi} + \left(R_s I_s - \frac{\Omega_s L_{\sigma s} I_s}{\sin\varphi}\cos\varphi\right)\cos\varphi + \sqrt{\left(\frac{E_{mN} f_s}{f_{sN}}\right) - \left(\left(R_s I_s\right) - \frac{\Omega_s L_{\sigma s} I_s}{\sin\varphi}\cos\varphi\right)^2 \sin^2\varphi} \qquad (7)$$

By compensating both resistive and reactive voltage drop, further improvements of the torque capability may be achieved.

V. SIMULATION RESULTS

There were performed simulations of current compensated constant Volt/Hertz operation according to equations (5) and (7). The nameplate rated data of the motor are: power P_N=2.2 kW, stator frequency f_{sN}=50 Hz, stator voltage U_{sN}=230/400 V, stator current I_{sN}=8.2/4.7 A, power factor cosφ= 0.82, and speed n_N=1420 rpm.

The motor was started under no-load condition. Than it was gradually loaded until breakdown torque was reached.

This procedure was repeated for different working frequencies below the rated one. The simulation results were obtained for a 15 Nm/s load torque variation.

Fig. 8 presents the simulated characteristics for different working frequencies, using both of the previously presented voltage-compensation methods.

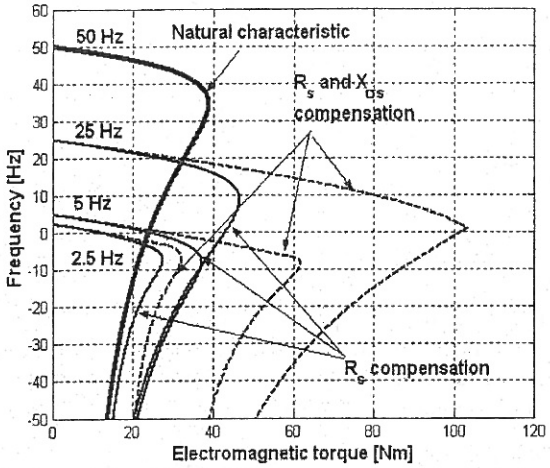

Fig. 8. Simulated artificial static mechanical characteristics for different frequencies

The natural characteristic at U_{sN} = ct. and f_{sN} is also plotted on this figure. It can be observed a substantial increase of the motor torque capability, especially for that particular case, if both the resistive and the reactive voltage drops are compensated. Note that even at 5Hz the linear part of the machine characteristic is greater than at rated frequency and also at 2.5 Hz the obtained characteristics are very close to it. At 25 Hz the sudden breakdown of the characteristics is due to the reason that the computed voltage has reached the rated value, and was not increased any more. Taking into account, that the characteristics were obtained by dynamic simulation, thus can be considered quasi-static ones.

Because most of the supplies cannot assure more than the rated voltage 230V to the motor phases, the compensation methods are "useless" at rated frequency or above. However, in order to analyze the possibilities of the presented voltage drop compensation methods, simulations were performed for an increased stator voltage value. The obtained simulation results are shown in Fig. 9.

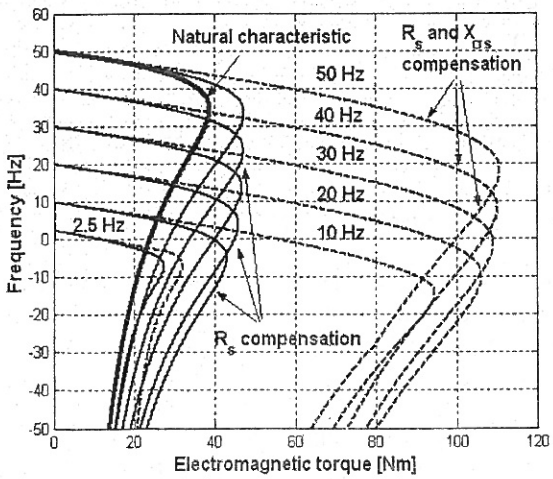

Fig. 9. Artificial mechanical characteristics at $U_s > U_{sN}$ for different frequencies

It can be observed that the increased breakdown torques for both methods are kept at constant level, only at low frequencies their value decreases. It is important to note, that during the dynamic simulation process (due to the continuous slow variation of the applied load torque), the obtained points on the characteristics are not exactly the corresponding steady-state working points. However, on the linear part of the mechanical characteristic the difference is not so critical, but beyond the breakdown torque value this difference is no more neglectable. It is also important to observe the variations of the stator and airgap fluxes versus the electromagnetic torque. At low working frequencies difficulties occurs in keeping the stator-flux at constant value.

In Fig. 10 for only resistive voltage drop compensation the stator-flux is indirectly kept constant at the rated value, while the air-gap flux decreases. The sudden change occurs only if the breakdown torque is reached, and the stator-flux magnitude is also dropping.

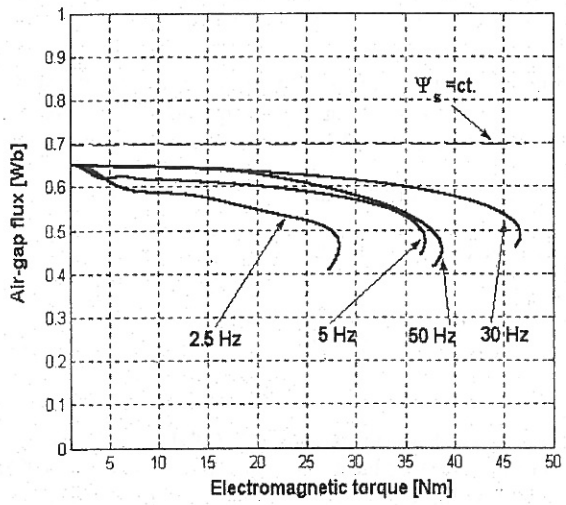

Fig. 10. Variation of the air-gap flux versus electromagnetic torque, at different working frequencies for resistive and reactive voltage-drop compensation

The rotor flux presents variations, as is shown in Fig. 11.

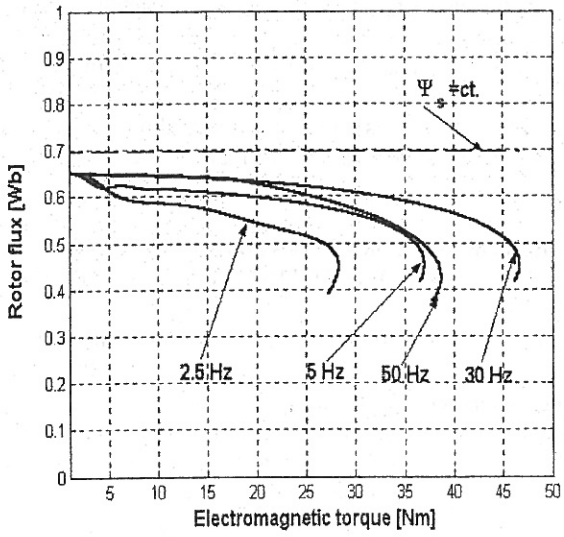

Fig. 11. Variation of the rotor flux versus electromagnetic torque at different working frequencies for resistive voltage-drop compensation

In the case of compensation method, when both the resistive and reactive voltage drops are compensated, the air-gap flux value will kept at constant level, while the stator-flux value will increase. At low frequencies and also beyond the breakdown point may be observed similar effects as in the previous case. The variation of the stator- and rotor-flux versus torque for this method (indirect Ψ_m control) is presented in Fig. 12 and Fig. 13, respectivelly.

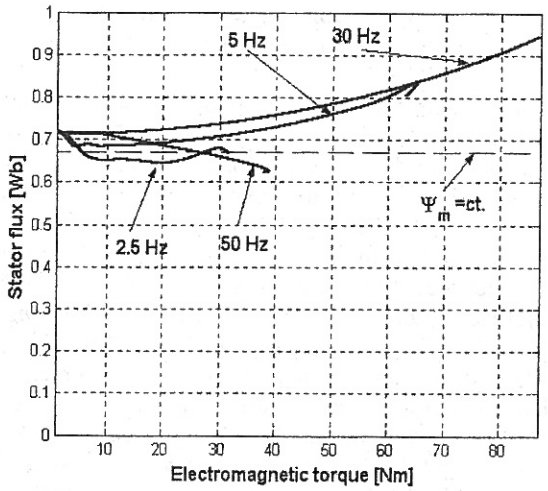

Fig. 12. Variation of the stator flux versus electromagnetic torque at different working frequencies for resistive and reactive voltage-drop compensation

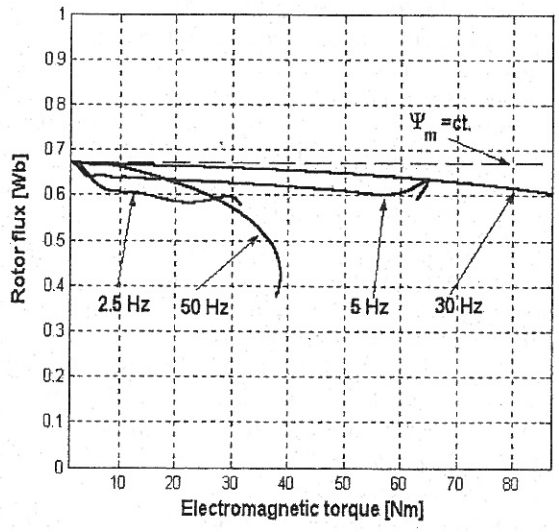

Fig. 13. Variation of the rotor flux versus electromagnetic torque at different working frequencies for resistive and reactive voltage-drop compensation

The simulation results presented in figures 10-13 shows that at rated frequency (f_{sN}=50 Hz) the effect of the stator voltage limitations (at U_{sN} = 230 V r.m.s): the flux values are kept at constant value until the rated torque is reached (15.8 Nm), after that it drops.

For a better analysis of the induction motor operation it is important to see the variation of the stator current versus torque, especially at the rated value. Fig 14 presents the variation of the absorbed stator current versus electromagnetic torque.

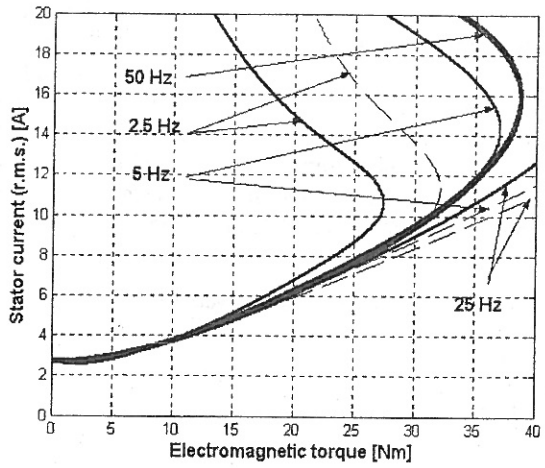

Fig. 14. Stator current versus torque

It can be observed that the stator currents are smaller if voltage drop compensation method is used. That means an optimized working condition from energetical point of view.

VI. EXPERIMENTAL RESULTS

Fig. 13 shows the structure of the experimental set-up, which is consisting of the tested induction motor drive (IM Type 1LA7-4AA10, SIEMENS) powered by a modified industrial DANFOSS inverter (type VLT5004), which is controlled by PC, via a dSPACE DS1104 controller card. The mechanical load machine is a SIEMENS permanent magnet synchronous machine (PMSM) driven in 4 quadrants by means of a SIMOVERT equipment configured in torque-control mode. It provides the measured actual speed and actual torque value, too.

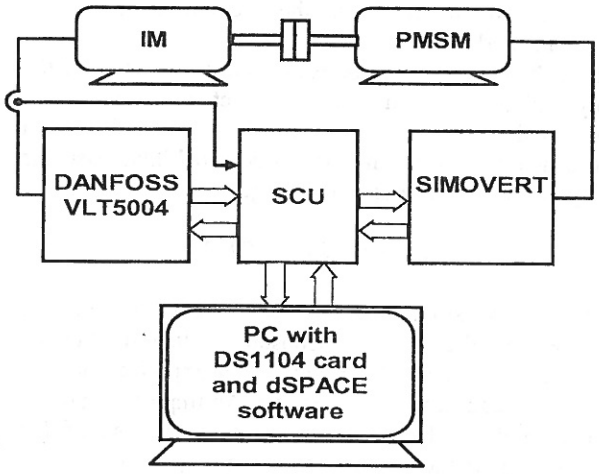

Fig. 13. Experimental set-up

The control signals and the acquisitioned data are conditioned and isolated galvanic by a Signal Conditioning Unit (SCU). The real-time software is running on RISC/DSP processors of the DS1104 card, and it is generated automatically based on MATLAB-Simulink files. The dSPACE has developed a specific Toolbox for Matlab. The controlling and monitoring tasks of real-time

experiments are provided by the "ControlDesk" experiment software.

Fig. 14 presents the experimental results for the classical Volt/Hertz method ("•" are measurement points), with no voltage-drop compensation, and for the R_s and $X_{\sigma s}$ compensation method ("x" are measurement points). Mechanical characteristics (torque-frequency) were traced based on the measurements for different working frequencies. For each case the motor was started under no-load condition, then different load torque was applied, up to 12 Nm.

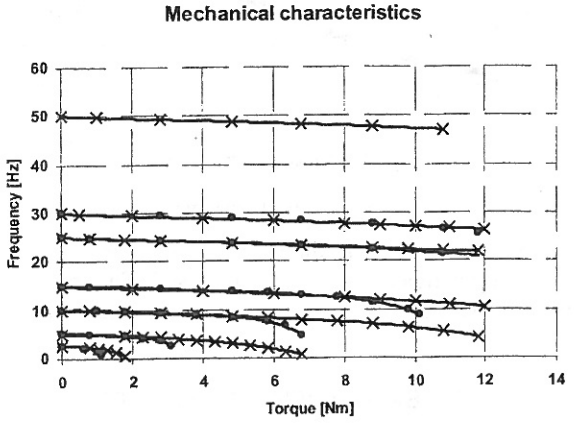

Fig. 14. Mechanical characteristics based on measurements

The experimental results show the improvement of the motor characteristics if the voltage-drop compensation method was applied. However, there are some differences between the experimental and the simulation results. These are due to the fact, that in simulation were not taken into account the voltage drops, which appear in the inverter (the internal resistance of the IGBT-s), in the three-phase supply cable (on the studied experimental rig is about 4 m long), and also were neglected the fluctuations of the DC-link voltage and the dead-time effect.

The voltage drops may be estimated up to 5-6% of the supply voltage, and due to the fact that voltage is proportional with the square of the torque, it has a significant effect on the motor torque capability. Also the rigidity of the characteristics is changed.

VII. CONCLUSIONS

Based on the simulation and experimental results, we concluded that the presented Constant Voltage-Frequency procedure is substantially improved by applying the two vectorial voltage-drop compensation. An important gain of these methods is that it makes possible the use of *U/f* procedure also in the low frequency region (2.5 Hz).

During experimental measurements we observed, that supplementary voltage drops appears on different components of the drive system (like the inverter, or the three-phase supply cable, etc.), which were not taken into account in this paper. Further improvements of the machine working characteristics may be made also by applying slip compensation. At very low speed some instability appears, therefore it was necessary to introduce a first-order leg for filtering the current dependent component of the stator-voltage computation.

VIII. ACKNOWLEDGMENT

Special thanks to Prof. Frede Blaabjerg and Assoc. Prof. Remus Teodorescu from Institute of Energy Technology, Aalborg University, and to the Danfoss Drives A/S, Denmark, for their generous support.

IX. REFERENCES

[1] A. Abbondanti, "Method of flux control in induction motors driven by variable frequency, variable voltage supplies," IEEE IAS Annual Meeting, 1977, pp 177-184,

[2] J. Holtz, "Methods for speed sensorless control of AC drives," (paper reprinted from IEEE PCC-Yokohama: 1993. pp. 415-420), in: *Sensorless Control of AC Drives*, a selected reprint volume, IEEE Press, New York: 1996, pp. 21-29.

[3] Maria Imecs, I. I. Incze, Cs. Szabo, T. Adam, "Scalar and vector-control structures of AC motors," *Conference of Energetics and Electrical Engineering, ENELKO 2003*, Cluj, Romania, 2003, pp. 82-98.

[4] Maria Imecs, Cs. Szabo, "Control structures of induction motor drives - state of the art," (Invited paper), *Proceedings of the 4th Workshop on European Scientific and Industrial Collaboration (Promoting: Advanced Technologies in Manufacturing) WESIC 2003*, Miskolc, Hungary, 2003, ISBN 963 661 570, pp. 495-510.

[5] Maria Imecs, "From scalar to vector control of AC drives," *Proceedings of the SIELMEN 2003,* Chisinau, Republica Moldova, 2003, pp 110-115.

[6] A. Kelemen, *Actionari Electrice*, Editura Didactica si Pedagogica, Bucuresti: 1979, p. 434 .

[7] A. Munoz-Garcia, T. A. Lipo, D. W. Novotny, "A new induction motor V/f control method capable of high-performance regulation at low speeds," *IEEE Transactions on Industry Applications:*, Vol. 34, No.4, July/Aug, 1998, pp. 813-821.

[8] K. Rajashekara, A. Kawamura, K. Matsuse, "Speed sensorless control of induction motors," in *Sensorless Control of AC Drives, A selected reprint volume.* IEEE Press, New York, 1996, pp. 1-19.

[9] R. Ueda, T. Sonoda, K. Koga; M. Ichikawa, Stability analysis in induction motor driven by V/f controlled general-purpose inverter, *IEEE Transactions on Industry Applications*, Vol. 28, No. 2, March/Apr, 1992, pp. 472-481.

[10] R. Teodorescu, M. Bech, *Course in Control of PWM Inverter-Fed Induction Machine*. Institute of Energy technology, Aalborg University, Denmark, 2000.

[11] I. I. Incze, Maria Imecs, Cs. Szabo, "Simple Voltage-Hertz Control With Current Feedback of the Induction Machine," in *Proceedings of 2004 IEEE-TTTC International Conference on Automation, Quality and Testing, Robotics, AQTR 2004 – THETA 14,* Cluj-Napoca, ISBN 973-713-046-4, Tome I, pp. 389-394.

[12] Maria Imecs, I. I. Incze, "A Simple Approach to Induction Machine Parameter Estimation," *Workshop on Electrical Machines Parameters,* 19 May 2001, Technical University of Cluj-Napoca, pp. 73-80.